Fish and Shellfish Immunology 103 (2020) 442–453

Contents lists available at ScienceDirect

Fish and Shellfish Immunology

journal homepage: www.elsevier.com/locate/fsi

Full length article

An effector caspase *Sp-caspase* first identified in mud crab *Scylla paramamosain* exhibiting immune response and cell apoptosis

Jishan Li[a,1], Lixia Dong[a,1], Depeng Zhu[a], Min Zhang[a], Kejian Wang[a,b,c], Fangyi Chen[a,b,c,*]

[a] State Key Laboratory of Marine Environmental Science, College of Ocean & Earth Sciences, Xiamen University, Xiamen, Fujian, China
[b] State-Province Joint Engineering Laboratory of Marine Bioproducts and Technology, Xiamen University, Xiamen, Fujian, China
[c] Fujian Collaborative Innovation Center for Exploitation and Utilization of Marine Biological Resources, Xiamen University, Xiamen, Fujian, China

ARTICLE INFO

Keywords:
Scylla paramamosain
Sp-caspase
Immune response
Apoptosis

ABSTRACT

Apoptosis plays a key role in the immune defense against pathogen infection, and caspase is one of the most important protease enzyme families, which could initiate and execute apoptosis. Among crustaceans, several caspase genes have been reported. However, caspase in mud crab *Scylla paramamosain*, have not been identified yet. Here, in the present study, we characterized a new caspase, named as *Sp-caspase*, from *S. paramamosain*. The full-length cDNA sequence of *Sp-caspase* contained 966 bp open reading frame, encoding 322 amino acids, and its molecular weight was 36 kDa. This gene has three conserved domains of the caspase family, a prodomain, a large subunit P20 and a small subunit P10. Phylogenetic analysis showed that *Sp-caspase* was clustered into an effector caspase group. *Sp-caspase* mainly distributed in midgut, hepatopancreas, hemocytes and female ovaries, and the transcript was significantly regulated in different tissues after being challenged with *Vibrio parahaemolyticus*, *Vibrio alginolyticus* or LPS. After infection with *V. alginolyticus*, the apoptosis rate of hemocytes notably increased, while the mRNA level of *Sp-caspase* and hydrolysis activity of caspase 3/7 significantly decreased. Furthermore, *in vitro* assays showed that the recombinant protein t*Sp*-caspase (deletion of *Sp*-caspase prodomain) could efficiently recognize and cleave human caspase 3/7 substrate Ac-DEVD-*p*NA, functioning as an effector caspase. Meanwhile, heterologous expression of *Sp*-caspase in several cell lines (HEK293T cells, HeLa cells and HighFive cells) could specifically induce cell apoptosis. Taken together, these data demonstrated that *Sp-caspase* could perform apoptosis as an effector caspase. In addition, it might be a negative regulator of hemocytes apoptosis under pathogen infection, which would contribute to homeostasis and immune defense of hemocytes in *S. paramamosain*.

1. Introduction

Apoptosis, also known as programmed cell death, plays essential roles in a variety of biological processes such as embryonic development, tissue remodeling, cell homeostasis [1,2]. Besides, apoptosis as an important evolutionarily conserved defense strategy from mammals to nematodes, can eliminate unnecessary, infected or damaged cells without causing inflammatory response or tissue damage and take part in the immune defense [1,2].

Caspases, cysteine-dependent aspartate-specific proteases, play a central role in the execution of apoptosis [3,4]. They are first synthesized as inactive zymogens [4,5], which contain three domains: a prodomain, a large subunit (P20) with conserved QACRG motif and a small subunit (P10) [6,7]. When caspase is activated, it will form heterodimer with two P20 and two P10 [8]. Caspases can be categorized into two subgroups based on their functions, the inflammatory caspases and the apoptotic caspases. The inflammatory caspases include caspase 1, 4, 5, 12 in humans and caspase 1, 11, 12 in mice [4,9], all of which contain a caspase activation and recruitment domain (CARD) [9]. Caspase 1, 4, 5 can cleave IL-1 family members and participate in innate immune responses, and caspase 11 and 12 are reported to be an activator and inhibitor of caspase 1, respectively [4]. As for the apoptotic caspases, they comprise initiator caspases (caspase 2, 8, 9, 10) and effector caspases (caspase 3, 6, 7) [4,6,9]. Initiator caspases, which have a long prodomain (> 90 amino acids), containing protein-protein interaction motifs such as the death effector domain (DED) or CARD, can activate effector caspases [8]. And effector caspases, which have a short prodomain (about 20–30 amino acids), can cleave cellular components and

* Corresponding author. State Key Laboratory of Marine Environmental Science, College of Ocean & Earth Sciences, Xiamen University, Xiamen, Fujian, 361102, China.
E-mail address: chenfangyi@xmu.edu.cn (F. Chen).
[1] These authors made equal contributions.

https://doi.org/10.1016/j.fsi.2020.05.045
Received 22 November 2019; Received in revised form 10 May 2020; Accepted 15 May 2020
Available online 21 May 2020

result in cell death [8].

Since the term of apoptosis was introduced in 1972 [8], hundreds of molecules involved in apoptosis have been revealed in many vertebrates, including 13 human caspases [10], 11 mouse caspases [10], 8 *Xenopus laevis* caspases [11,12] and 14 zebra fish caspases [13,14]. Besides, apoptosis-related molecules and signaling pathways were also studied in invertebrates, such as *Caenorhabditis elegans* [15] and *Drosophila melanogaster* [16,17]. In *C. elegans*, CED-3, CED-4, CED-9, EGL-1 were demonstrated to be the core cell death members and take part in the genetic pathway during apoptosis [15]. As for *D. melanogaster*, there were seven molecules involving in the apoptotic process, including Dronc, Dredd, Strica, DrICE, Dcp-1, Decay and Damm [16,17].

In aquaculture animals, many efforts have been made to identify more caspase family members and to reveal their immune functions upon pathogen infection. Till now, caspase 6 [18] and caspase 7 [19] from pufferfish (*Takifugu obscurus*), caspase 3 [20] and caspase 9 [21] from large yellow croaker (*Pseudosciaena crocea*), caspase 3 [22] from rock bream (*Oplegnathus fasciatus*), caspase 1, 2, 3, 9 [23] from tongue sole (*Cynoglossus semilaevis*), caspase 1, 3, 9 [24] from miiuy croaker (*Miichthys miiuy*), caspase 6 [25] and caspase 8 [26] from sea cucumber (*Holothuria leucospilota*), caspase 1 [27] from sea cucumber (*Apostichopus japonicus*), caspase 1 [28], similar to vertebrate caspase-3/7, from oyster (*Crassostrea gigas*), and caspase 3 [29] from oyster (*C. gigas*), abcaspase [30] from colored abalone (*Haliotis diversicolor*) are characterized and supposed to be involved in antibacterial or antiviral mechanisms.

In crustaceans, several initiator caspases and effector caspases have been characterized. *Pm*Casp [31,32] and *Pm*caspase [33] from *Penaeus monodon*, *Pj*Caspase [34,35] from *Marsupenaeus japonicas*, CAP-3 [36] from *Penaeus merguiensis*, and *Lv*caspase 2–5 (*Lv*caspase 2 and *Lv*caspase 5 as effector caspases, *Lv*caspase 3 and *Lv*caspase 4 as initiator caspases) [37] from *Litopenaeus vannamei* were found to be involved in the immune defense process of WSSV infection. In addition, *ES*-Casp [38] and *Es*Caspase-3-like [39] from *Eriocheir sinensis* responded to *Vibrio anguillarum* and microbial polysaccharide (LPS, peptidoglycan and zymosan) stimulation, respectively. In *Portunus trituberculatus*, *Pt*Cas 2, 3, 4 [40] were identified and their pathogen induced expression pattern upon WSSV, *Vibrio alginolyticus* and *Vibrio parahaemolyticus* infection were analyzed. All these studies revealed that caspases of crustaceans played important roles in immune defense process upon bacterial and viral infection.

Mud crab *Scylla paramamosain* is an economically important species in aquaculture and is widely cultured in southeast coastal region of China. However, compared to other aquaculture species, there is no caspase gene reported from *S. paramamosain* yet. Besides, the apoptosis associated molecules and their underlying mechanisms remain to be fully elucidated [41]. In this study, a new caspase from *S. paramamosain*, named as *Sp-caspase*, was cloned. Tissue distribution and the expression patterns of this gene upon *V. parahaemolyticus*, *V. alginolyticus* infection and LPS stimulation were revealed. Apoptosis rate and the hydrolysis activity of caspase 3/7 in hemocytes upon *V. alginolyticus* infection were detected to investigate the immune function of *Sp-caspase*. In addition, *in vitro* assays, the hydrolysis activity of recombinant proteins was analyzed and heterologous expression in several cell lines (HEK293T cells, HeLa cells and HighFive cells) were performed to reveal its apoptotic characteristics.

2. Materials and methods

2.1. Experimental animals, sample collection and immune challenge

Healthy male and female crabs (*S. paramamosain*) with average weight 300 ± 50 g were purchased from a local market in Xiamen, Fujian Province, China. Before the experiments, the crabs were reared in tanks at 25 ± 2 °C for several days.

Different tissues (including heart, midgut, gills, hepatopancreas, brain, stomach, thoracic ganglion, testis, seminal vesicle, ejaculatory duct, posterior ejaculatory duct, ovaries, spermatheca, reproductive tract, muscle, eyestalks) were sampled from five random individuals for total RNA isolation. Hemolymph was mixed with equal volume of sterile anti-coagulant solution (NaCl 450 mM, glucose 100 mM, citric acid 26 mM, trisodium citrate 30 mM, EDTA 10 mM, pH 4.6) and centrifuged at 4 °C, 500 g for 10 min to obtain the hemocytes [42].

As for immune challenge experiment, only male crabs were selected since many papers mentioned that estrogen in female was a mitogen, which could promote cell growth and inhibit apoptosis through estrogen receptor (ER)-mediated mechanisms [43–46]. In the experiment, male crabs were randomly separated into six groups and each group contained 40 crabs. The three experimental groups were injected with 100 μL of 1.2×10^7–4.8×10^7 cfu/mL *V. alginolyticus* (CGMCC 1.1833) or 100 μL of 3.6×10^7 cfu/mL *V. parahaemolyticus* (CGMCC 1.1997) or 100 μL of 5 mg/mL LPS (Sigma-Aldrich, St. Louis, MO, USA) from *Escherichia coli* serotype O55:B5 in base of the fourth leg in the right side of crabs. Both the LPS and bacteria were diluted with sterile modified crab saline solution (NaCl 496 mM, KCl 9.52 mM, $MgSO_4$ 12.8 mM, $CaCl_2$ 16.2 mM, $MgCl_2$ 0.84 mM, $NaHCO_3$ 5.95 mM, HEPES 20 mM, pH 7.4). The three control groups were injected with 100 μL crab saline solution. Different tissues (including midgut, hemocytes, hepatopancreas and gills) were collected at 0 h, 3 h, 6 h, 12 h, 24 h, 48 h, 72 h and 96 h post injection as described previously.

2.2. RNA and genomic DNA isolation and cDNA synthesis

Total RNA was isolated from different tissues with TRIzol Reagent (Life Technologies, Gaithersburg, MD, USA). The integrity of RNA was assessed through agarose gel electrophoresis and the concentration and quality of RNA was analyzed by NanoDrop 2000 spectrophotometer (Thermo Fisher Scientific, Waltham, MA, USA). The genomic DNA was extracted from muscle tissue using Universal Genomic DNA Extraction Kit Ver.3.0 (TaKaRa, Tokyo, Japan) following the manufacturer's instructions. The cDNA was synthesized using PrimeScript RT reagent Kit with gDNA Eraser (TaKaRa, Tokyo, Japan). The 5′ and 3′ RACE-ready cDNA were prepared using SMART RACE cDNA Amplification Kit (Clontech, Mountain View, CA, USA).

2.3. Cloning the full-length cDNA sequence and genomic DNA sequence of Sp-caspase

Partial cDNA sequence of *Sp-caspase* was obtained from the embryonic transcriptome library of mud crab *S. paramamosain*. Specific primers (Casp-F/Casp-R) were designed to amplify the intermediate cDNA sequence of *Sp-caspase*. And primers (Casp3′F, SMARTIIA oligo, 3′-CDS Primer A, 5′-RACE CDS Primer A) were synthesized to clone the 5′ and 3′ cDNA ends of *Sp-caspase*. Four pairs of specific primers (GeneF1/GeneR1, GeneF2/GeneR2, GeneF3/GeneR3, GeneF4/GeneR4) were used to amplify the genomic DNA. Sequences of primers were listed in Table 1.

2.4. Bioinformatics analysis

DNAMAN ver.8.0 software (Lynnon Biosoft, San Ramon, CA, USA) was used to analyze the deduced amino acid sequence and generate multiple alignment of amino acid sequences. The theoretical molecular weight (MW) and isoelectric point (PI) were calculated by DNAssist 2.2 program (Patterton and Graves 2000 [47]). Functional protein domains were predicted at https://prosite.expasy.org/. Neighbor-joining phylogenetic tree of amino acid sequences were constructed using MEGA ver.6.0 software (Tamura, Stecher, Peterson, Filipski and Kumar 2013 [48]), and the reliability was tested using bootstrap resampling (1000 pseudo-replicates).

Table 1
Sequences of primers used in this study.

Primers	Sequences (5′–3′)
Casp-F	CTGGTTAACTCATACACTTGCGAAG
Casp-R	GTTGATGGCTGTCCTGAGATGTT
Casp3′F1	GCTGACTGTAGCTGCCAGATGTG
Casp3′F2	CGAGCTTTCAGATGTCAGTGGCTG
Casp3′F3	GAGGTGATGTGTGTTAGGTTGGCATG
SMART IIA oligo	AAGCAGTGGTATCAACGCAGAGTACGCGGG
3′-CDS Primer A	AAGCAGTGGTATCAACGCAGAGTAC(T)30VN (N = A, C, G, T; V = A, G, C)
5′-CDS Primer A	(T)25VN (N = A, C, G, T; V = A, G, C)
GeneF1	CTGGTTAACTCATACACTTGCGAAG
GeneR1	GCATAGCGGAGAGACTCAGCAGCCG
GeneF2	GAATCTGGGCTGGTCTCTAATTTGGC
GeneR2	CTTGTAGGCTAATCGTCCCGAGTC
GeneF3	CTTCCAAGCAGATCAGTGCAAGTC
GeneR3	GGTGTTGCGCCAGGAATAGTG
GeneF4	GTGTTAATCTGGTCCGCACTCG
GeneR4	GTTGATGGCTGTCCTGAGATGTT
rt-CASP-F	GTGTTAATCTGGTCCGCACTCG
rt-CASP-R	GGTGTTGCGCCAGGAATAGTG
BOK-F	GAGAAAGTCTTCCATGCCCATAG
BOK-R	ATCTTCCTGGTGACATCGCTCA
Bcl2-F	GATGCGACGACTGGATGTG
Bcl2-R2	TCTTCTCGGTGCAGTGTAAGG
IAP-F	GCAGAACAGGCTCTCAATGCTG
IAP-R	GAGGAGGATGAGCCAAGAGTAGC
rt-GAPDH-F	CTCCACTGGTGCCGCTAAGGCTGTA
rt-GAPDH-R	CAAGTCAGGTCAACCACGGACACAT
cDNA-Spcaspase-F	AGGAGGAAGACCATAGAGG
cDNA-Spcaspase-R	GCCTAAGATGACATGTTTGC
T7-Spcaspase-F	TAATACGACTCACTATAGGGGGCTTTGAACATCCAGTGTTG
T7-Spcaspase-R	TAATACGACTCACTATAGGG CGCTTCTTGTGAGACCCT
rt-T7-F	TGTCAACGGCTGCTGAGTC
rt-T7-R	CACCTTTACCTGGTCTCTGTC
T7-GFP-F	TAATACGACTCACTATAGGGCGACGTAAACGGCCACAAGT
T7-GFP-R	TAATACGACTCACTATAGGGTTCTTGTACAGCTCGTCCATGC
P20-28a-F	CATGCCATGGGCCTCCGCTATGCAGGGTCTCAC
P20-28a-R	CCGCTCGAGTCAATGGTGATGGTGATGATGGTCTATTTCATCAATATGGCGAG
P10-28a-F	CATGCCATGGGCTCGGGACGATTAGCCTACAAG
P10-28a-R	CCGCTCGAGTCAATGGTGATGGTGATGATGCTTTGGGGCCAGGTAAACC
pCMVHA-CASP-F	CGGAATTCCAGAGAATGTCAAGGGAAATG
pCMVHA-CASP-R	CCGCTCGAG TCAATACTTTGGGGCCAGGTAA
pIZ-CASP-F	CGGAATTCAGAATGGAGAATGTCAAGGGAAATG
pIZ-CASP-R	CCGCTCGAGATACTTTGGGGCCAGGTAA
pmCherry-CASP-F	CCGCTCGAGCTGAGAATGTCAAGGGAAATG
pmCherry-CASP-R	CGGGATCCTCAATACTTTGGGGCCAGGTAA

2.5. Expression profiles of Sp-caspase and apoptosis-related genes

The expression profiles of *Sp-caspase* and apoptosis-related genes were analyzed on Applied Biosystems 7500 Real-Time PCR system with 7000 system SDS software ver.1.3.1 (Applied Biosystems, Foster City, CA, USA) using FastStart Universal SYBR Green Master (Roche, Basel, Switzerland). Gene Specific primers (rt-CASP-F/rt-CASP-R, BOK-F/BOK-R, Bcl2-F/Bcl2-R, IAP-F/IAP-R) were designed to perform qPCR, and the relative expression levels were normalized to *GAPDH* gene (its specific primers: rt-GAPDH-F/rt-GAPDH-R). The amplification reaction was set as follows: 50 °C for 2 min, 95 °C for 10 min, 40 cycles of 95 °C for 15 s, and 60 °C for 1 min. DEPC water instead of templates was used as a negative control. The gene expression profiles were calculated using $2^{-\Delta\Delta CT}$ method [49]. Sequences of primers were listed in Table 1.

2.6. RNA interference assay

RNAi assay was conducted with double-strand RNA (dsRNA) to inhibit the mRNA level of *Sp-caspase* in primary cultured hemocytes of *S. paramamosain*. The template DNA and target sequence for dsRNA synthesis were prepared with different pairs of primers (cDNA-Spcaspase-F/cDNA-Spcaspase-R, T7-Spcaspase-F/T7-Spcaspase-R). The detection primers for RNAi efficiency were rt-T7-F/rt-T7-R. The dsRNA was synthesized with MegaScript kit (Ambion, Austin, TX, USA) according to the manufacturer's instructions and purified with TRIzol Reagent (Life Technologies, Gaithersburg, MD, USA). Sequences of primers were listed in Table 1.

The hemocytes (10^6 cells/mL) were grown and maintained in 24-well plates with Leibovitz's L15 medium (pH 6.3) (Thermo Fisher Scientific, Waltham, MA, USA) with 0.2 M NaCl at 23 °C. Transfection was conducted using Lipofectamine 2000 (Invitrogen, Carlsbad, CA, USA) with a final concentration of 1 μg/mL dsRNA according to the manufacturer's instructions. The GFP dsRNA (primers: T7-GFP-F/T7-GFP-R) was used as a negative control. The hemocytes were collected at 24 h and 36 h for further analysis.

2.7. Annexin V-FITC/PI staining in hemocytes upon V. alginolyticus infection

The apoptosis rate of hemocytes after *V. alginolyticus* infection was detected using Annexin V-FITC Apoptosis Detection Kit (DOJINDO, Kumamoto, Japan) according to the manufacturer's instructions. Briefly, after bacterial injection, hemocytes were collected at 3 h, 6 h, 12 h, 24 h, 48 h and 72 h as described previously, and washed twice with Leibovitz's L15 medium (pH 6.3) (Thermo Fisher Scientific, Waltham, MA, USA) containing 5% fetal bovine serum (FBS) (Gibco

BRL, Grand Island, NY, USA) and 0.2 M NaCl, then centrifuged at 4 °C, 500 g for 10 min. The hemocyte pellets were then resuspended in 1 × Annexin V Binding Solution to obtain a final density of 1×10^6 cells/mL. 100 μL sample was stained with 5 μL Annexin V-FITC and 5 μL PI at room temperature and incubated in dark for 15 min. 400 μL 1 × Annexin V Binding Solution was added to each sample and apoptosis rate was analyzed using CytoFLEX flow cytometer with CytoFLEX ver.2.0 software (Beckman Coulter, Brea, CA, USA) and laser scanning confocal microscopy (LSM780NLO, Carl Zeiss, Jena, Germany) with ZEN 2011 software.

2.8. Hydrolysis activity in hemocytes upon V. alginolyticus infection

Hemocytes after *V. alginolyticus* infection were collected at 3 h, 6 h, 12 h, 24 h, 48 h and 72 h as described previously. Total proteins of hemocytes were extracted with 100 μL lysis buffer (25 mM HEPES, 5 mM MgCl2, 5 mM EDTA, 5 mM dithiothreitol, 2 mM phenylmethylsulfonyl fluoride, pH7.5), which were homogenized on ice for 15 min and centrifuged at 12,000 g, 4 °C for 15 min [20,21]. Protein concentration was detected with Bradford Protein Assay Kit (Beyotime, Shanghai, China) according to the manufacturer's instructions and adjusted to 2 mg/mL with lysis buffer. The hydrolysis activity was performed using Caspase-Glo 3/7 Assay (Promega, Madison, WI, USA) according to the manufacturer's instructions.

2.9. Expression and purification of recombinant tSp-caspase, P20 and P10

The cDNA sequence of functional domains of *tSp-caspase* (deletion of *Sp-caspase* prodomain), P20 and P10 were inserted into pET-28a expression vector (Novagen, Madison, WI, USA) with C-terminal His-Tag using specific primers (P20-28a-F/P10-28a-R, P20-28a-F/P20-28a-R, P10-28a-F/P10-28a-R, listed in Table 1). The recombinant plasmids were transformed into Transetta (DE3) (TransGen Biotech, Beijing, China) and induced with 0.5 mM Isopropyl *β*-D-Thiogalactoside (IPTG) when optical density (OD_{600}) was 0.5–0.6 at 28 °C, 160 rpm in LB culture medium. The lysates were collected and purified with protein elution buffer (50 mM Na_2HPO_4, 300 mM NaCl, 250 mM imidazole, pH 8.0) using HIS-Select Nickel Magnetic Agarose Beads (Sigma-Aldrich, St. Louis, MO, USA) according to the manufacturer's instructions. Purified protein concentration was detected using Pierce BCA Protein Assay Kit (Thermo Fisher Scientific, Waltham, MA, USA). About 0.5–2 μg purified proteins were boiled with 1 × SDS loading buffer (10% *β*-mercaptoethanol included) and then subjected to SDS-PAGE gel. The major bands were excised from the gel, divided into 1.5 mm × 1.5 mm pieces, digested with trypsin, and analyzed using mass spectrometer (timsTOF Pro, Bruker Daltonics, Bremen, Germany), which was operated by engineers at School of Life Sciences (Xiamen University).

2.10. Hydrolysis activity of recombinant tSp-caspase, P20 and P10

In vitro hydrolysis activity was performed using Caspase-Glo 3/7 Assay (Promega, Madison, WI, USA), Caspase-Glo 8 Assay (Promega, Madison, WI, USA), and Caspase-Glo 9 Assay (Promega, Madison, WI, USA) according to the manufacturer's instructions. Briefly, equilibrate the caspase buffer and caspase substrates to room temperature and mix them well until the substrates were dissolved thoroughly to form the working reagent. Add 50 μL of working reagent to an equal volume of different amounts of protein, 12.5 ng and 6.25 ng of t*Sp*-caspase, and 10 μg, 5 μg and 2.5 μg of both P20 and P10 domain. Protein elution buffer was used as a negative control. Gently mix the plate and incubate it at room temperature for 30 min. And then record the luminescence (Infinite F200 PRO, Tecan, Maennedorf, Switzerland) with Tecan i-control ver.3.4 software every 15 min, 180 min in total. The experiments were repeated three times.

As for the relative hydrolysis activity analysis, luminescence intensity detected with three different caspase substrates subtracting their negative control was normalized to luminescence intensity on caspase 9 substrate Ac-LEHD-*p*NA, and shown as fold change [20,39]. And the formulas (RHA is relative hydrolysis activity, L is luminescence, three caspase substrates are abbreviated to DEVD, LETD and LEHD) were shown as follows:

$$RHA_{DEVD} = \frac{L_{DEVD}\ (Protein) - L_{DEVD}\ (Buffer)}{L_{LEHD}\ (Protein) - L_{LEHD}\ (Buffer)} \quad (1)$$

$$RHA_{LETD} = \frac{L_{LETD}\ (Protein) - L_{LETD}\ (Buffer)}{L_{LEHD}\ (Protein) - L_{LEHD}\ (Buffer)} \quad (2)$$

$$RHA_{LETD} = \frac{L_{LEHD}\ (Protein) - L_{LEHD}\ (Buffer)}{L_{LEHD}\ (Protein) - L_{LEHD}\ (Buffer)} \quad (3)$$

2.11. Cell culture and plasmid transfection

HeLa and HEK293T cells (10^5-10^6 cells/mL) were grown and maintained with DMEM/high glucose (Thermo Fisher Scientific, Waltham, MA, USA) with 10% FBS (Gibco BRL, Grand Island, NY, USA) and 1% penicillin-streptomycin liquid (Thermo Fisher Scientific, Waltham, MA, USA) in a cell incubator (37 °C, 5% CO_2). HighFive cells (10^6 cells/mL) were cultured with Sf-900 II SFM (Thermo Fisher Scientific, Waltham, MA, USA) at 28°C in a cell incubator. All the cells were cultured in 24-well plates overnight and then transfected with recombinant plasmids.

The open reading frame (ORF) sequence of *Sp-caspase* was amplified with different pairs of primers (pCMVHA-CASP-F/pCMVHA-CASP-R, pIZ-CASP-F/pIZ-CASP-R, pmCherry-CASP-F/pmCherry-CASP-R, listed in Table 1) and the PCR products were inserted into pCMVHA Vector (Clontech, Mountain View, CA, USA), pIZV5-His Vector (Invitrogen, Carlsbad, CA, USA) and pmCherry-C1 Vector (Clontech, Mountain View, CA, USA), respectively. Recombinant plasmids were prepared using endotoxin-free plasmid extraction kit (TianGen, Beijing, China) following the manufacturer's instructions. Lipofectamine 3000 (Invitrogen, Carlsbad, CA, USA) was used for pCMVHA/*Sp*-caspase and pmCherry-C1/*Sp*-caspase transfection. In 24-well plates, 1 μg recombinant plasmids was mixed with 1 μL P3000 Reagent and 1 μL Lipofectamine 3000 Reagent. And Cellfectin Reagent (Thermo Fisher Scientific, Waltham, MA, USA) was used for pIZV5-His/*Sp*-caspase transfection. In 24-well plates, 1 μg recombinant plasmids was mixed with 2 μL Cellfectin Reagent. The cells were collected at 20 h, 40 h, 60 h and 80 h post transfection for western blotting.

2.12. Western blotting analysis

Transfected cells at different time points in section 2.11 were washed with PBS (NaCl 137 mM, KCl 2.7 mM, Na_2HPO_4 10 mM, KH_2PO_4 2 mM, pH7.4), resuspended in 1 × SDS loading buffer (10% *β*-mercaptoethanol included), boiled for 10 min and then about 50–100 μg protein was loaded into each well of SDS-PAGE gel, which was adjusted according to the band of *β*-actin. Proteins were transferred to PVDF membranes and blocked with 5% Difco skim milk (BD Becton Dickinson, Franklin Lakes, NJ, USA) in TBS (Tris 10 mM, NaCl 150 mM, pH7.4) with 0.1% Tween-20. The membranes were incubated with primary antibodies, Anti-HA Tag rabbit polyclonal antibody (dilution of 1:1000, Sangon Biothch, Shanghai, China), Mouse Anti-His mAb (dilution of 1:1000, ZSGB-BIO, Beijing, China), Mouse Anti-*β*-actin mAb (dilution of 1:5000, ZSGB-BIO, Beijing, China), followed by incubating with HRP-conjugated Goat Anti-Rabbit IgG (dilution of 1:8000, Sangon Biothch, Shanghai, China), HRP-conjugated Goat Anti-Mouse IgG (dilution of 1:8000, Sangon Biothch, Shanghai, China). Immobilon Western Chemiluminescent HRP Substrate (EMD Millipore, Billerica, MA, USA) was used to detect the positive bands in chemiluminescent imaging system (Tanon 5200S, Tanon, Shanghai, China) with FLICapture

ver.1.02 software.

2.13. Annexin V-FITC/Hoechst staining in HEK293T cells

Early apoptosis analysis was detected in HEK293T cells with Annexin V-FITC Apoptosis Detection Kit (DOJINDO, Kumamoto, Japan) according to the manufacturer's instructions. Briefly, transfected HEK293T cells in section 2.11 were collected at 24 h, resuspended with 1 × Annexin V Binding Solution in cell culture medium to obtain a final density of 10^6 cells/mL, and stained with 5 μL Annexin V-FITC and 5 μL Hoechst in dark for 1 h. Apoptotic cells were analyzed using a laser scanning confocal microscopy (LSM780NLO, Carl Zeiss, Jena, Germany) with ZEN 2011 software.

2.14. TUNEL staining in cell lines

Late apoptosis analysis was detected in cell lines (HEK293T cells, HeLa cells and HighFive cells) with TUNEL (TdT-mediated dUTP nick end labeling) method using In Situ Cell Death Detection Kit (Roche, Basel, Switzerland) on the slide according to the manufacturer's instructions. Briefly, transfected cells in section 2.11 were fixed with 4% paraformaldehyde in PBS at room temperature for 30 min and then washed with PBS. Cells were permeabilized with 0.1% Triton X-100 in 0.1% sodium citrate for 2 min on ice and washed with PBS. 5 μL Enzyme solution was added to 45 μL Label Solution to obtain 50 μL TUNEL reaction mixture. Cells were incubated with 50 μL TUNEL reaction mixture at 37 ˚C for 1 h in a humidified atmosphere in dark. Slides were rinsed with PBS. Label Solution and DNase I recombinant instead of TUNEL reaction mixture were added as negative control and positive control, respectively. After that, cells were counterstained with DAPI (0.5 μg/mL, Beyotime, Shanghai, China) for 10 min and analyzed using a laser scanning confocal microscopy (LSM780NLO, Carl Zeiss, Jena, Germany) with ZEN 2011 software.

2.15. Statistical analysis

PASW Statistics ver.18.0 software (IBM, Armonk, NY, USA) was used for statistical analysis. Student's *t*-test was carried out to determine the statistically significant and $p < 0.05$ (*) or $p < 0.01$ (**) was considered to be significant. Data were shown as mean ± standard deviation.

3. Results

3.1. Molecular cloning and characterization of Sp-caspase

Here, we cloned a complete cDNA sequence (GenBank accession number: KX151140) (Fig. 1A) and a genomic DNA sequence (GenBank accession number: KX151141) (Fig. 1B) of *Sp-caspase*. The full-length cDNA sequence of *Sp-caspase* included 966 bp ORF, 350 bp 5′ untranslated region (UTR) and 1511 bp 3′ UTR (Fig. 1A). It was predicted that *Sp-caspase* gene encoded 322 amino acids, and the molecular weight was 36 kDa. ScanProsite analysis of the deduced amino acid sequence of the *Sp-caspase* showed that it was comprised of a prodomain, P20 domain with the active site (pentapeptide QACRG motif) and P10 domain. The genomic DNA of *Sp-caspase* was 6382 bp in length and contained 8 exons and 7 introns, whose organization was shown in Fig. 1B.

3.2. Phylogenetic analysis

A neighbor-joining phylogenetic tree was constructed with caspase homologs in different species to analyze the evolutionary relationships of *Sp-caspase* (Fig. 1C). The results showed that caspases were categorized into two groups: the inflammatory caspases and the apoptotic caspases. And *Sp-caspase* was grouped to be an apoptotic caspase and clustered in a sub-group with other effector caspases.

3.3. Multiple sequence alignment

To further confirm the classification of *Sp-caspase*, multiple sequence alignment was carried out with several crustacean effector caspases. As shown in Fig. 1D, *Sp-caspase* shared relatively high amino acid sequence identity with *E. sinensis* caspase-3/7-1 (72.76%) and *Penaeus vannamei* caspase-2 (61.92%), and the identity with *P. vannamei* caspase-5, *P. monodon Pm*Casp and *P. merguiensis* CAP-3 ranged from 27.22% to 32.77%.

3.4. Tissue distribution of Sp-caspase

Tissue distribution of *Sp-caspase* was detected using qPCR. As shown in Fig. 2, *Sp-caspase* gene was widely expressed in all tested tissues and highly expressed in midgut, hepatopancreas, hemocytes and female ovaries, but low expression in muscle and heart.

3.5. Sp-caspase responded to LPS and V. parahaemolyticus challenge

To investigate the potential immune functions of *Sp-caspase*, the mRNA levels were determined upon LPS and bacterial challenge. After being infected with *V. parahaemolyticus*, the expression level of *Sp-caspase* significantly increased in midgut at 12 h, 48 h, 96 h post infection (hpi) and gills at 6, 12 hpi, whereas decreased in hemocytes at 24, 48 hpi. (Fig. 3A). When stimulated with LPS, *Sp-caspase* mRNA levels in midgut (at 24 hpi), hemocytes (at 6 hpi), hepatopancreas (at 12 hpi) and gills (at 12, 96 hpi) were notably upregulated (Fig. 3B).

3.6. Sp-caspase and apoptosis-related genes were involved in immune defense process of S. paramamosain upon V. alginolyticus infection

The mRNA level of *Sp-caspase* and apoptosis-related genes in hemocytes upon *V. alginolyticus* infection were also detected. As shown in Fig. 4A, the expression level of *Sp-caspase* in hemocytes significantly decreased at 24, 48 and 72 hpi. And the pro-apoptotic gene (*BOK*) and anti-apoptotic genes (*Bcl2* and *IAP)* were significantly up-regulated at 3 or 6 hpi (Fig. 4B–D). These results suggested that apoptosis-related genes were involved in the immune defense process of *S. paramamosain* under *V. alginolyticus* infection.

3.7. V. alginolyticus infection would promote hemocytes apoptosis of S. paramamosain

We further investigated the apoptosis rate in crab hemocytes upon *V. alginolyticus* infection with flow cytometry and confocal microscopy. As shown in Fig. 5A and Fig. 5B, the percentage of apoptotic hemocytes significantly increased at 48 and 72 hpi, indicating a higher proportion of Annexin V-FITC staining (green fluorescence) and PI staining (red fluorescence) (Fig. 5C). In addition, the hydrolysis activity of caspase 3/7 in hemocytes was notably reduced at 12 hpi (Fig. 5D), which corresponded to the mRNA level of *Sp-caspase* in hemocytes (decreased expression at 24, 48 and 72 hpi) (Fig. 4A). These results suggested that *V. alginolyticus* infection would result in serious damage to hemocytes and promote hemocytes apoptosis. On the other hand, the *Sp-caspase* might be a negative regulator of hemocytes apoptosis under pathogen infection, which would contribute to homeostasis and immune defense of hemocytes in *S. paramamosain*.

3.8. Expression and purification of recombinant tSp-caspase, P20 and P10

In order to assess the hydrolysis activity of *Sp*-caspase, the sequences of t*Sp*-caspase (without the prodomain, but with P20 and P10 domain), P20 domain and P10 domain were constructed into pET-28a vector with 6 × his tag at the C-terminal and expressed in *E. coli*. The

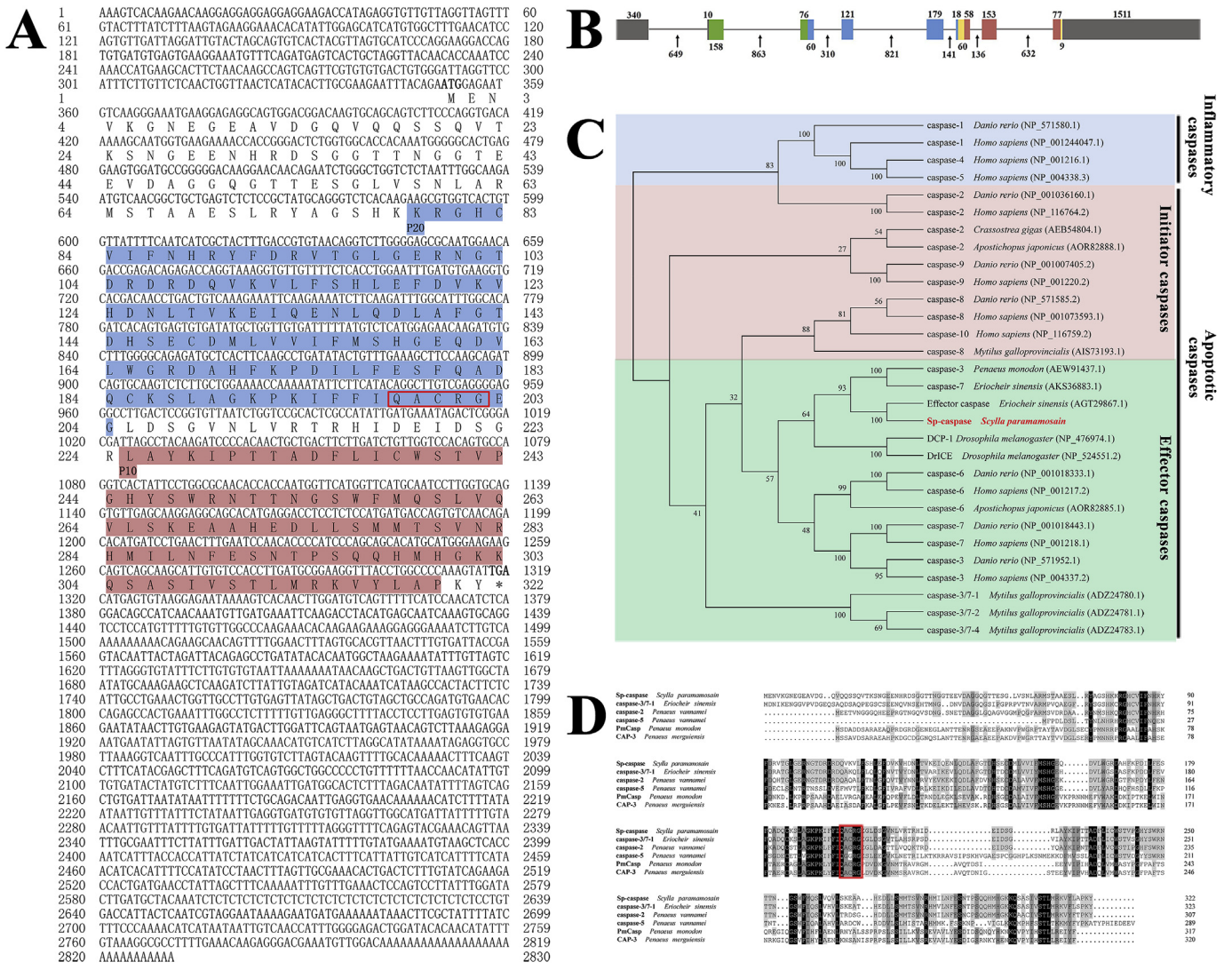

Fig. 1. The sequence analysis of *Sp-caspase*. (A) The cDNA sequence and the predicted amino acid sequence of *Sp-caspase*. The GenBank accession number of *Sp-caspase* is KX151140. The large domain P20 and the small domain P10 were highlighted in blue and red colour, respectively. The conserved active-site motif QACRG was in red line box. The stop codon was indicated by an asterisk. (B) The genomic DNA organization of *Sp-caspase*. The exons and introns were shown by colour boxes and gray lines, respectively. The numbers above or below the boxes indicated the length of exons, and the numbers with arrows represented the length of introns. The length of exons and introns was drawn to scale. The gray boxes represented for 5′ UTR or 3′ UTR. Prodomain was in the green boxes, P20 in the blue boxes, and P10 in the red boxes. The yellow boxes represented for linkers between domains. (C) Phylogenetic tree of *Sp-caspase*. A neighbor-joining phylogenetic tree of caspases was constructed using MEGA ver.6.0 software with 1000 bootstrap replications. *Sp-caspase* was shown in red. (D) Multiple amino acid sequence alignment of *Sp-caspase*. The GenBank accession numbers of crustacean effector caspases were listed as follows: *E. sinensis* caspase-3/7-1 (AGT29867.1), *P. vannamei* caspase-2 (AGL61581.1), *P. vannamei* caspase-5 (AGL61583.1), *P. monodon PmCasp* (ABI34434.1), *P. merguiensis* CAP-3 (AAX77407.1). The conserved active-site motif QACRG was highlighted in red line box. Identical and similar residues were indicated in black and gray, respectively. (For interpretation of the references to colour in this figure legend, the reader is referred to the Web version of this article.)

recombinant proteins were purified and the concentrations were determined. As shown in Fig. 6A, t*Sp*-caspase in SDS-PAGE gel showed three major bands with molecular mass of about 27 kDa, 15 kDa and 12 kDa. The band of 27 kDa corresponded with the t*Sp*-caspase, and the other two bands resulted from auto-processing of t*Sp*-caspase corresponded with the P20 and P10, which was confirmed by mass spectrometry analysis (Fig. S1). As for P20 and P10 recombinants, they showed a major single band with molecular mass around 15 kDa (Fig. S2A) and 12 kDa (Fig. S2D), respectively.

3.9. Recombinant t*Sp*-caspase showed caspase 3/7 hydrolysis activity

The hydrolysis activity assay of recombinant t*Sp*-caspase, P20 domain and P10 domain were then performed using various amounts of recombinant proteins against different caspase substrates. For t*Sp*-caspase (Fig. 6B), when the protein concentration was 6.25 ng, the luminescence intensity value on the caspase 3/7 substrate (Ac-DEVD-*p*NA) was higher than 200,000, but for the caspase 8 substrate (Ac-LETD-*p*NA) or caspase 9 substrate (Ac-LEHD-*p*NA), the value was less than 2,000, as low as the control group. In addition, when the protein concentration of t*Sp*-caspase increased to 12.5 ng, the luminescence intensity value on the caspase 3/7 substrate (Ac-DEVD-*p*NA) reached to 600,000, while the caspase 8 substrate (Ac-LETD-*p*NA) and caspase 9 substrate (Ac-LEHD-*p*NA) did not exceed 4,000. And for the P20 domain (Fig. S2B) or P10 domain (Fig. S2E), even when the protein amount was increased to 10 μg, the luminescence intensity value for all three caspase substrates were less than 4,000.

As for the relative hydrolysis activity, as shown in Fig. 6C, when t*Sp*-caspase was incubated with the caspase 3/7 substrate (Ac-DEVD-*p*NA), the relative hydrolysis activity was more than 700-fold, whereas there

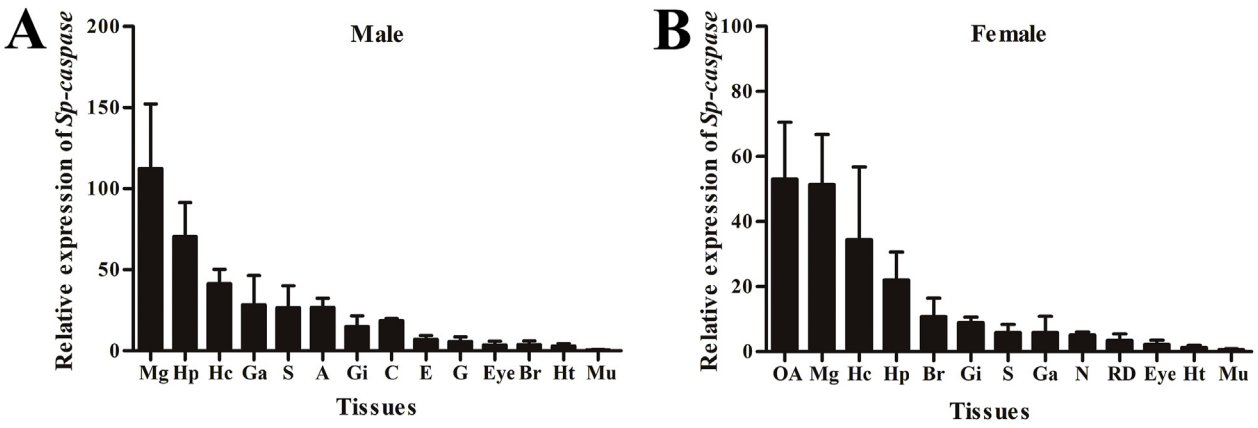

Fig. 2. Tissue distribution of *Sp-caspase* in both male (A) and female (B) crabs. The *GAPDH* gene was used as an internal control. Vertical bar represented the mean ± SD (n = 5). Mg, midgut; Hp, hepatopancreas; Hc, hemocytes; Ga, thoracic ganglion; S, stomach; A, testis; Gi, gills; C, seminal vesicle; E, ejaculatory duct; G, posterior ejaculatory duct; Eye, eyestalks; Br, brain; Ht, heart; Mu, muscle; OA, ovaries; N, spermatheca; RD, reproductive tract.

was no significant hydrolysis activity observed on the caspase 8 substrate (Ac-LETD-*p*NA) or caspase 9 substrate (Ac-LEHD-*p*NA). As for P20 domain (Fig. S2C), the relative hydrolysis activity on the caspase 3/7 substrate (Ac-DEVD-*p*NA) was only about 30-fold, and the activity on the other two caspase substrate was lower than 5-fold. As for P10 domain (Fig. S2F), it showed no apparent relative hydrolysis activity on all three caspase substrates.

3.10. Heterologous expression of Sp-caspase inducing apoptosis in different cell lines

In order to analyze the apoptosis activity of *Sp*-caspase, pCMVHA/*Sp*-caspase recombinant plasmid was transfected into HEK293T cells. *Sp*-caspase could be detected at 20 h post transfection by western blotting (Fig. 7A), and it could cause obviously morphological changes, including cell shrinkage, membrane blebbing, and the formation of apoptotic bodies (Fig. 7B). The same results were also shown in HeLa cells (Fig. S3A-B) and HighFive cells (Fig. S4A-B).

Annexin V-FITC/Hoechst staining was used to detect apoptosis at the early stage. In Fig. 7C, *Sp*-caspase could be successfully expressed in HEK293T cells, showing red fluorescence. The results revealed that the adherent property of cells was affected and cells changed to round. In addition, *Sp*-caspase notably induced a higher proportion of Annexin V-FITC staining (green fluorescence) and Hoechst staining (blue fluorescence), indicating that cells underwent apoptosis. As for the control group, cells appeared to have a normal adherent property and the integrity of cell membrane was not affected, which showed no apoptosis.

Sp-caspase was also overexpressed in HEK293T cells and then tested with TUNEL assay under the fluorescence microscope to detect apoptosis at the late stage. As shown in Fig. 7D, cells transfected with *Sp*-caspase showed significant characteristics of apoptosis (green fluorescence). The same results were also shown in HeLa cells (Fig. S3C) and HighFive cells (Fig. S4C).

4. Discussion

Mud crab *S. paramamosain* lacks adaptive immune system and mainly relies on innate immunity, including humoral and cellular immune responses [50]. It is reported that a high mortality caused by pathogens, especially vibrios and viruses, often occurs in mud crabs farm and this would hinder the development of the crab farming industry [41]. Therefore, elucidation of potential immune mechanisms and immune-related components is important for disease control. Till now, immune-related receptors, signaling pathways, antimicrobial proteins, reactive oxygen species (ROS) generation and the antioxidant system have been investigated in *S. paramamosain* [41], while the apoptosis-related caspase genes have not been reported yet.

In this study, we identified and characterized a new apoptosis-related gene, *Sp-caspase*, from mud crab *S. paramamosain*. We obtained the full-length cDNA sequence and the genomic DNA sequence of *Sp-caspase*. Motif analysis showed that *Sp-caspase* had conserved active site of QACRG and contained prodomain, P20 and P10 domain, which shared high similarity with other known caspase members [6,7]. Phylogenetic analysis showed that *Sp-caspase* was clustered in a sub-group with other effector caspases including caspase-7 [51] and effector caspase (caspase-3/7-1) [52] from *E. sinensis*. Besides, multiple sequence alignment indicated that *Sp-caspase* shared high amino acid identity with caspase-3/7-1 (72.76%) [52] from *E. sinensis* and caspase-2 (61.92%) [37] from *P. vannamei*, both of which were effector caspases. Cluster of phylogenetic tree and sequence identity analysis would be associated with protein function, and these results indicated that *Sp-caspase* might take part in apoptotic signaling pathway as an effector caspase in *S. paramamosain*.

Tissue expression analysis revealed that *Sp-caspase* mRNA was widely distributed in all tested tissues, and this expression pattern was the same as other effector caspases such as Lyccasp3 in *P. crocea* [20], Rbcasp3 in *O. fasciatus* [22], *Mn*caspase-3c in *Macrobrachium nipponense* [53], *Pm*caspase in *P. monodon* [33], *Aj*caspase-3 in *A. japonicus* [54] and *Es*Caspase-3-like in *E. sinensis* [39]. *Sp-caspase* was also found to be highly expressed in midgut, hepatopancreas, hemocytes and female ovaries, which was similar to several other species. For example, *Aj*-caspase-3 in *A. japonicus* [54] was abundant in intestine, and *Mr*Casp3c in *Macrobrachium rosenbergii* [55] was expressed at a high level in both hepatopancreas and hemocytes. In addition, *Es*Caspase-3-like [39] and caspase-3/7-1 [52] in *E. sinensis*, *Pt*Cas 3 [40] in *P. trituberculatus* and *Mn*caspase-3c [53] in *M. nipponense* were highly expressed in hemocytes. Tissue distribution results suggested that *Sp-caspase* might function in different tissues.

To further investigate the immune functions of *Sp-caspase*, the expression profiles after immune challenge were investigated. LPS is the main component of the cell wall of gram-negative bacteria and can activate immune response. Under the stimulation of LPS, mRNA levels of *Sp-caspase* in midgut, hemocytes, hepatopancreas and gills were significantly up-regulated. Similar results were observed in *E. sinensis* hemocytes, in which the transcripts of *Es*Caspase-3-like increased at 2 h, 6 h and 12 h [39] and the expression level of caspase-3/7-1 increased at 6 h, 12 h, 24 h, 48 h after LPS stimulation [52]. *Vibrio* spp., which could be isolated from crabs, shrimps, shellfish, fish, etc., is one of the major pathogenic bacteria in aquaculture [56–59]. Upon *V. parahaemolyticus* challenge, the mRNA levels of *Sp-caspase* in midgut and gills were significantly up-regulated. However, the expression profiles of *Sp-caspase* in hemocytes was significantly down-regulated at 24 h, 48 h or 72 h

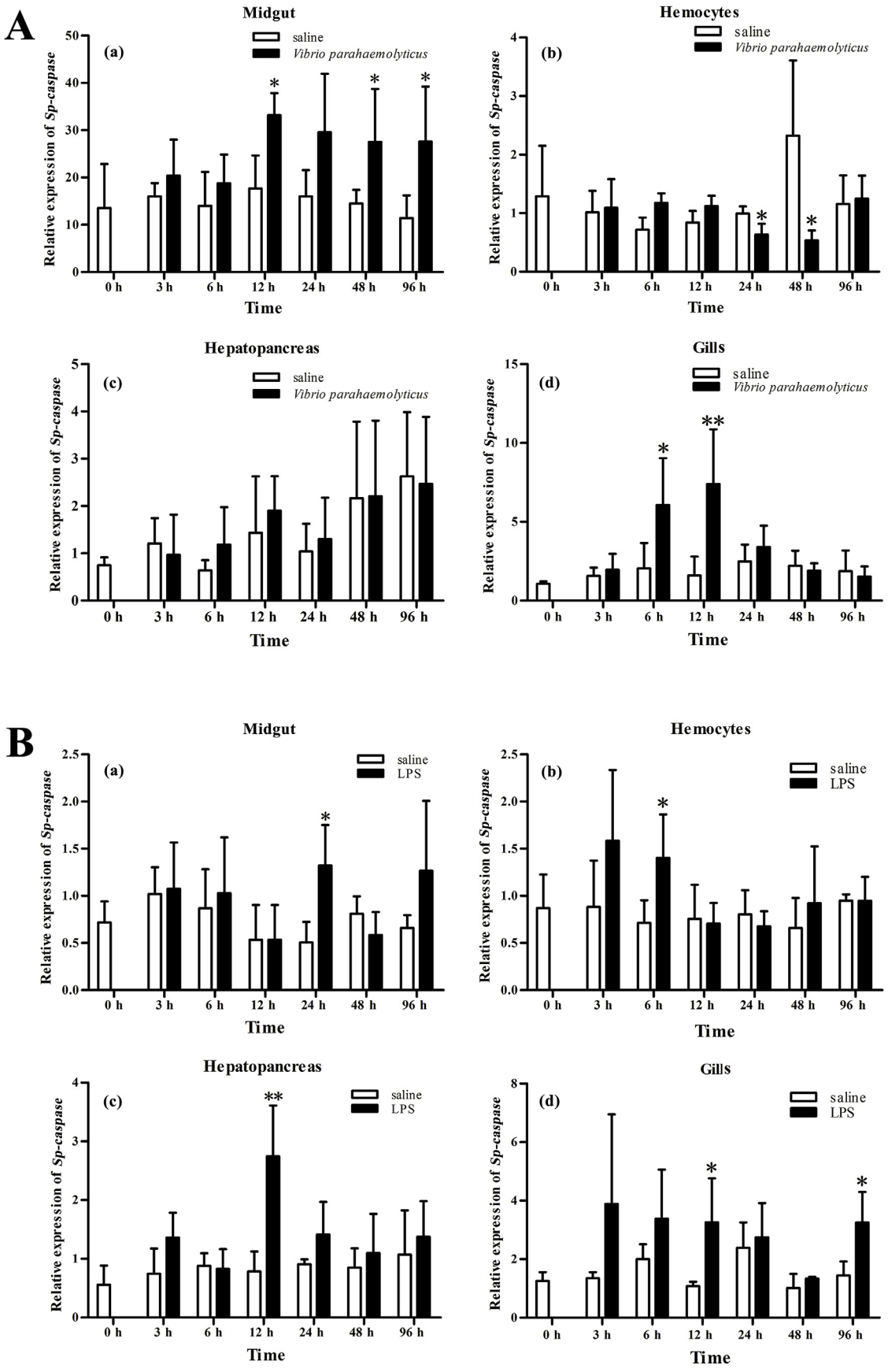

Fig. 3. Expression profiles of *Sp-caspase* in midgut, hemocytes, hepatopancreas and gills after being challenged with *V. parahaemolyticus* (A) and LPS (B). The control groups were injected with sterile crab saline solution. The *GAPDH* gene was used as an internal control. Vertical bar represented the mean ± SD (n = 5). $p < 0.05$ (*) or $p < 0.01$ (**) was considered to be significant difference.

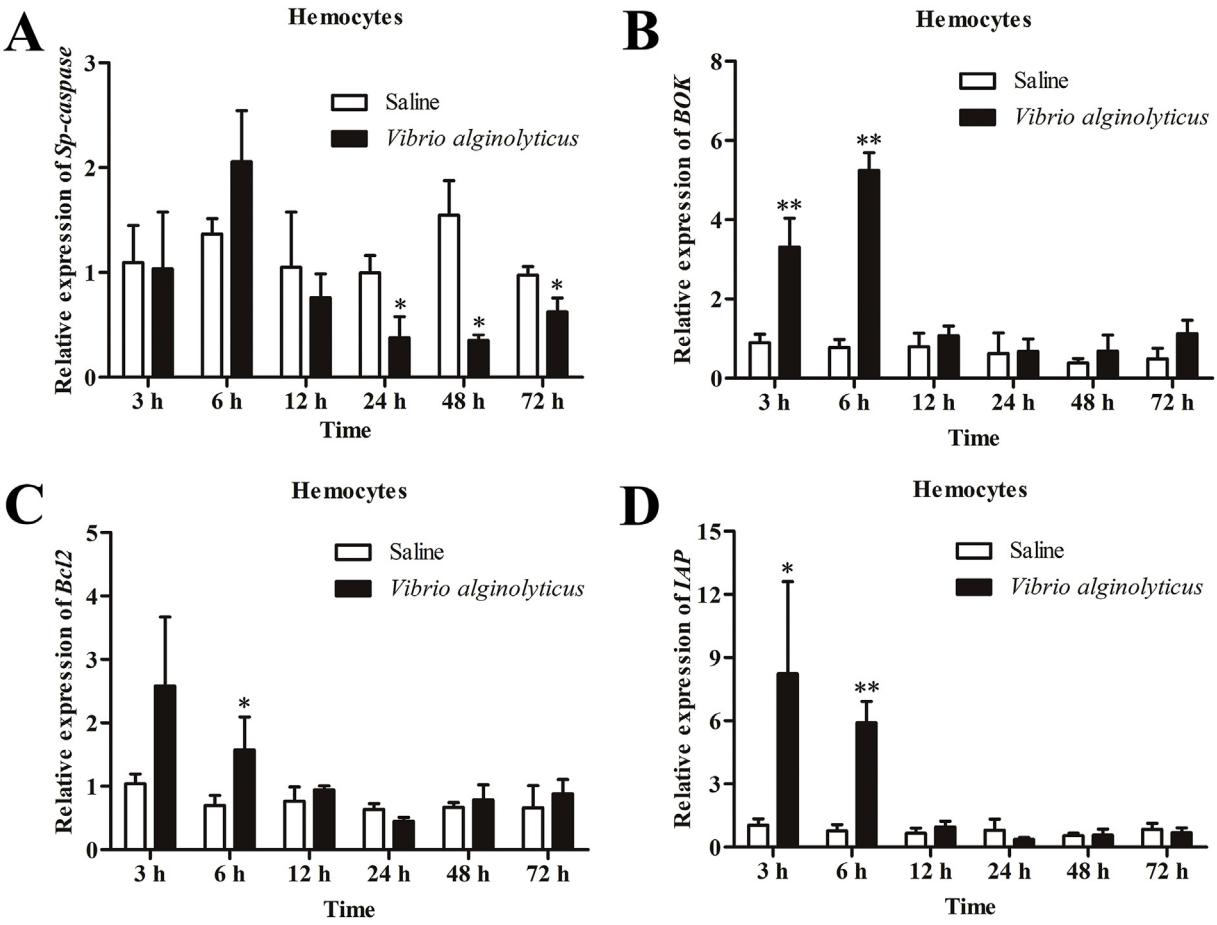

Fig. 4. Expression profiles of *Sp-caspase* (A) and apoptosis-related genes including *BOK* (B), *Bcl2* (C) and *IAP* (D) in hemocytes upon *V. alginolyticus* infection. The control groups were injected with sterile crab saline solution. The *GAPDH* gene was used as an internal control. Vertical bar represented the mean ± SD (n ≥ 3). $p < 0.05$ (*) or $p < 0.01$ (**) was considered to be significant difference.

upon both *V. parahaemolyticus* and *V. alginolyticus* infection. The caspase 3/7 hydrolysis activity of crab hemocytes corresponded to the mRNA level of *Sp-caspase*, which was notably reduced at 12 hpi.

We also selected several key components of apoptotic signaling pathway, including pro-apoptotic gene (*BOK*) and anti-apoptotic genes (*Bcl2* and *IAP*), to investigate whether they are involved in the immune response of *S. paramamosain* under bacterial challenge. In addition, RNAi assay was performed to study whether *Sp-caspase* would affect the expression of these genes. The results showed that *BOK*, *Bcl2* and *IAP* were significantly regulated after infection. And when the efficiency of RNA interference for *Sp-caspase* was about 34% at 24 h post transfection, the mRNA expression level of *Bcl2* and *IAP* significantly decreased and increased, respectively (Fig. S5). These results suggested that the three apoptotic signaling pathway related genes were involved in the immune defense process of *S. paramamosain* under *V. alginolyticus* infection and *Sp-caspase* would affect the gene expression of *Bcl2* and *IAP*.

Meanwhile, we detected the apoptosis rate in hemocytes of *S. paramamosain* post *V. alginolyticus* infection and the results showed that the percentage of apoptotic hemocytes increased significantly at 48 and 72 hpi. In previous study, it was reported that the number of hemocytes in *S. paramamosain* dramatically declined at 24 h upon *V. alginolyticus* challenge [60], which was consistent with our results.

The results of apoptosis detection and expression pattern analysis suggested that bacterial infection would result in serious damage to hemocytes and promote hemocytes apoptosis. On the other hand, the *Sp-caspase* might be regulated through apoptotic signaling pathway and be a negative regulator of hemocytes apoptosis under pathogen infection, which would contribute to homeostasis and immune defense in *S. paramamosain*. However, the involved mechanism still needs further investigation.

In order to assess the caspase activity of *Sp*-caspase *in vitro*, t*Sp*-caspase was expressed by prokaryotic expression system. And our result showed that t*Sp*-caspase has self-cleavage properties and could produce P20 and P10, which was confirmed by mass spectrometry analysis. However, the recombinant products were tagged with 6 × His tag only at C-terminal, thus, when anti-His antibody was used for western blotting analysis, t*Sp*-caspase and P10 formed by self-cleaved would appear positive bands, but not P20. And the positive band of P20 might be due to poor antibody specificity. The auto-processing property of caspase was also reported in previous findings [28,61]. In *Spodoptera frugiperda*, the recombinant *Sf* caspase-1 could produce three products P19, P18 and P12, with molecular mass of about 19 kDa, 18 kDa and 12 kDa, respectively [61]. And in oyster *Crassostrea giga*, the recombinant *Cg*Caspase-1 zymogen could produce Pro, P20P10 and P10 [28].

When the hydrolysis activity of recombinant t*Sp*-caspase was detected, it showed high enzyme activity against human caspase 3/7 substrate (Ac-DEVD-*p*NA), which was similar to other effector caspases from *P. crocea* [20], *E. sinensis* [39,52] and *M. nipponense* [53]. These results demonstrated that *Sp*-caspase could execute apoptosis as an effector caspase. To further study the apoptosis activity, *Sp*-caspase was overexpressed in cell lines. The results showed that heterologous expression of *Sp*-caspase in HEK293T cells, HeLa cells and HighFive cells could induce apoptosis with typical morphological features, which was the same as *Cg*caspase-3 [29] in oyster *C. gigas*, *Pm*caspase [33] in *P. monodon* and DCP-1 [62] in *D. melanogaster*.

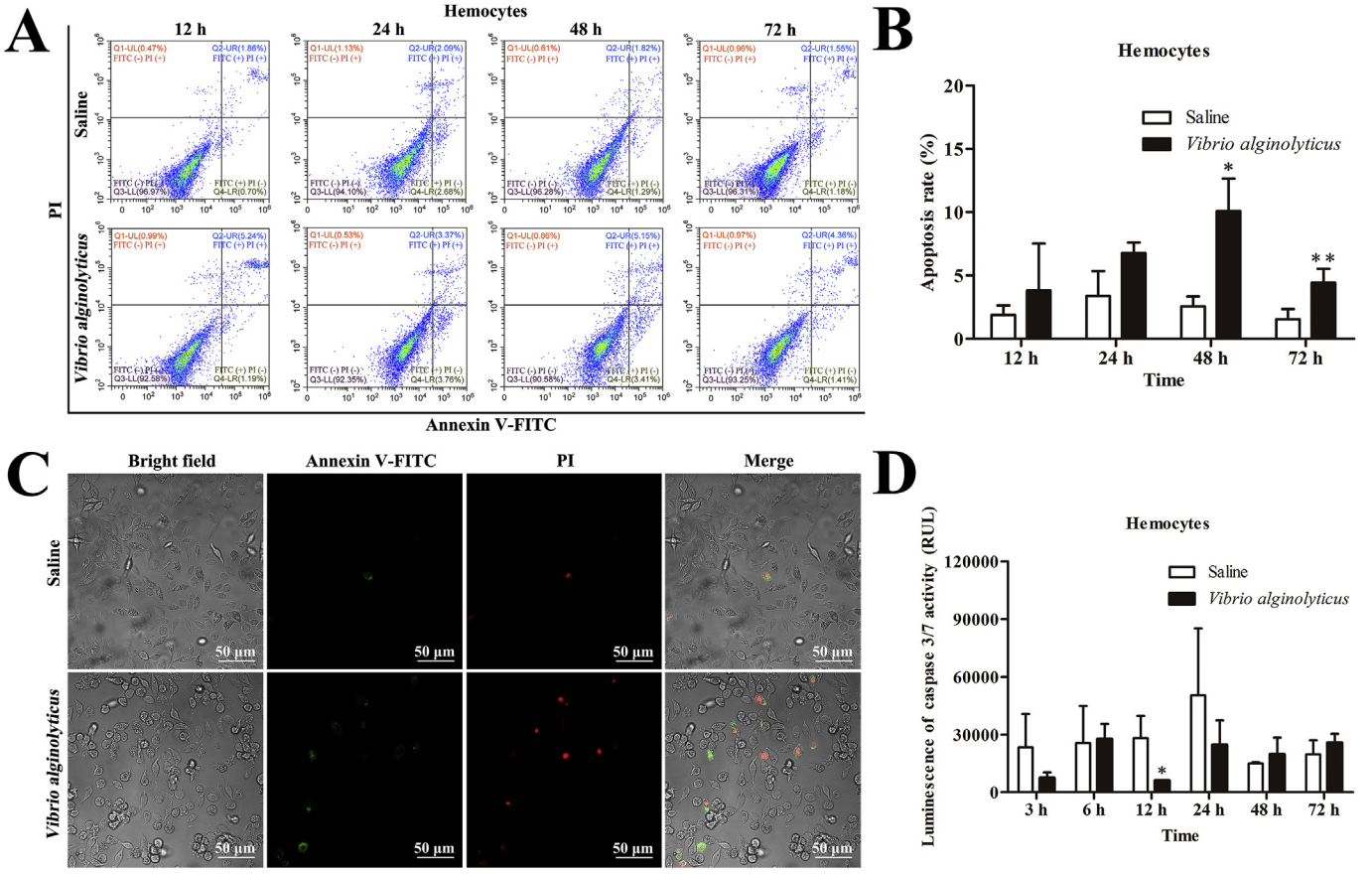

Fig. 5. Apoptosis detection in hemocytes upon *V. alginolyticus* infection. (A) Flow cytometric analysis of Annexin V-FITC/PI stained hemocytes upon *V. alginolyticus* infection. Viable cells (Annexin V-FITC − /PI −), early apoptotic cells (Annexin V-FITC + /PI −) and late apoptotic cells (Annexin V-FITC + /PI +) are located in Q3, Q4 and Q2, respectively. (B) Apoptosis rate of hemocytes upon *V. alginolyticus* infection. (C) Confocal microscopy analysis of Annexin V-FITC/PI stained hemocytes upon *V. alginolyticus* infection. Bacterial infection caused apoptosis in hemocytes and induced a higher percentage of Annexin V-FITC staining (green fluorescence) and PI staining (red fluorescence). Scale bar = 50 μm. (D) The hydrolysis activity of caspase 3/7 in hemocytes after being challenged with *V. alginolyticus*. Vertical bar represented the mean ± SD (n ≥ 3). $p < 0.05$ (*) or $p < 0.01$ (**) was considered to be significant difference. (For interpretation of the references to colour in this figure legend, the reader is referred to the Web version of this article.)

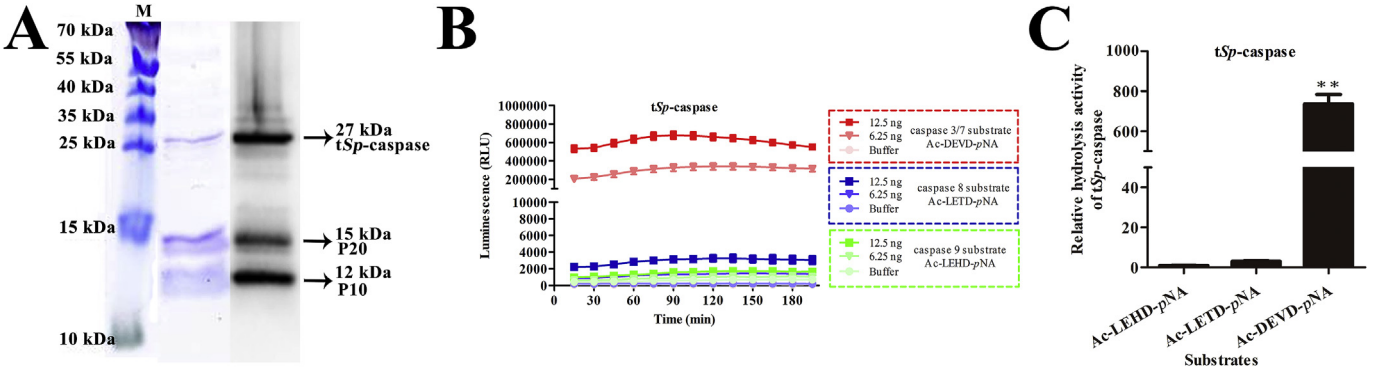

Fig. 6. Expression, purification and hydrolysis activity analysis of recombinant t*Sp*-caspase. (A) Expression and purification of recombinant t*Sp*-caspase. The samples were subjected to SDS-PAGE and stained with Coomassie Brilliant Blue R-250 or detected by western blotting. Molecular mass of the three major bands were about 27 kDa, 15 kDa and 12 kDa. (B) The hydrolysis activity of t*Sp*-caspase. Recombinant t*Sp*-caspase in different amounts were detected with caspase 3/7 substrate Ac-DEVD-*p*NA, caspase 8 substrate Ac-LETD-*p*NA and caspase 9 substrate Ac-LEHD-*p*NA to determine the hydrolysis activity. The buffer was also measured as a negative control. (C) The relative hydrolysis activity of t*Sp*-caspase. Recombinant t*Sp*-caspase was detected with caspase 9 substrate Ac-LEHD-*p*NA, caspase 8 substrate Ac-LETD-*p*NA and caspase 3/7 substrate Ac-DEVD-*p*NA when the protein amount was 12.5 ng at the time point of 90 min. The hydrolysis activity was normalized to activity of t*Sp*-caspase on caspase 9 substrate Ac-LEHD-*p*NA and shown as fold change. $p < 0.05$ (*) or $p < 0.01$ (**) was considered to be significant difference. (For interpretation of the references to colour in this figure legend, the reader is referred to the Web version of this article.)

In conclusion, our study provided a fundamental knowledge of a potential immune-related molecule, *Sp-caspase*, which was demonstrated to be an effector caspase and it might be a negative regulator of hemocytes apoptosis under pathogen infection, which would contribute to homeostasis and immune defense in *S. paramamosain*. However, the study of apoptosis in crustaceans is still in infancy. There are many questions need to be answered. Firstly, apoptosis in organisms is precisely regulated by a complex network comprising hundreds of genes,

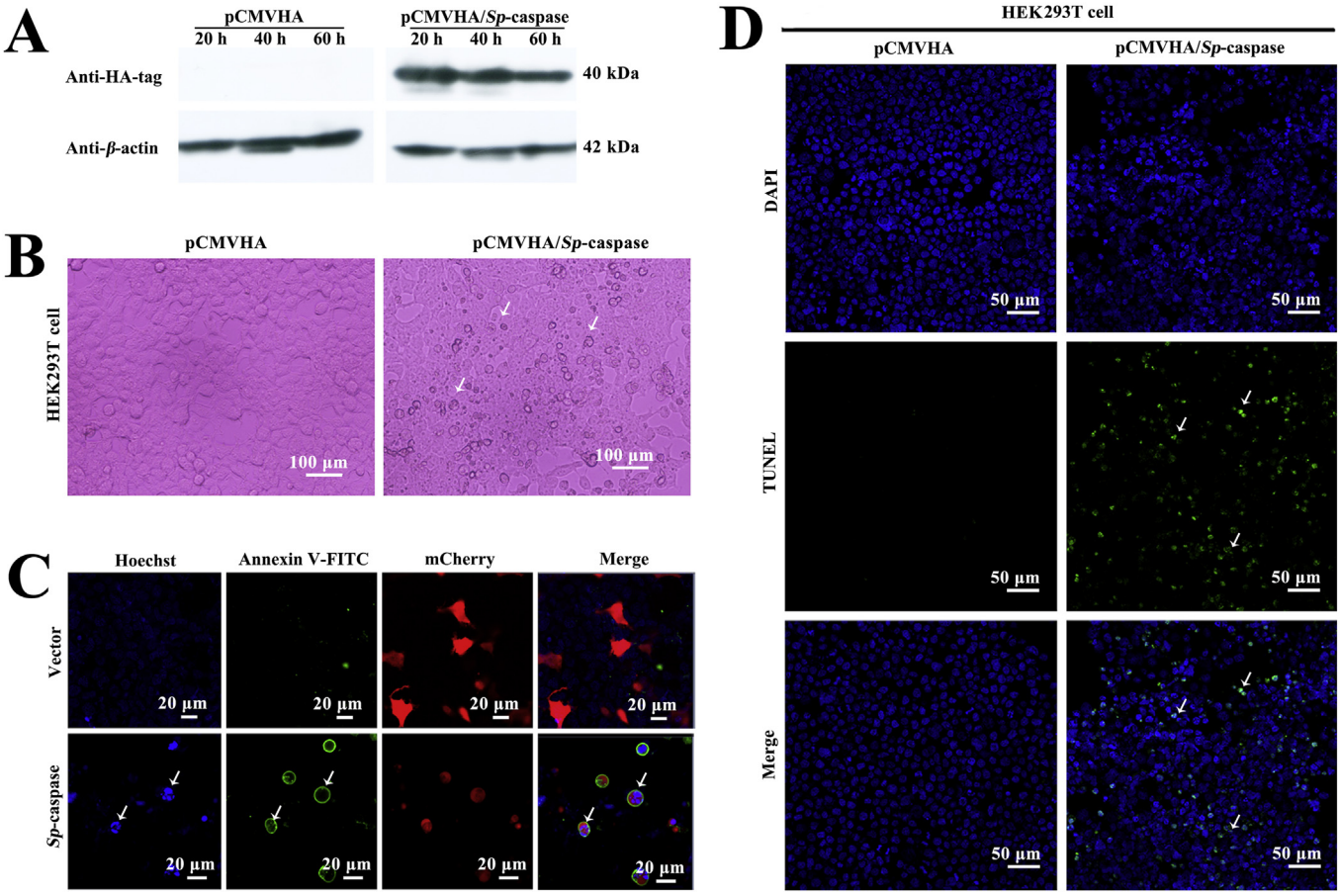

Fig. 7. Apoptosis detection when *Sp*-caspase was expressed in HEK293T cells. (A) The protein expression of *Sp*-caspase in HEK293T cells at different time post transfection was analyzed by western blotting. *β*-actin was used as a loading control. (B) Overexpression of *Sp*-caspase caused morphological changes in HEK293T cells. White arrows indicated the apoptotic cells with obviously morphological changes. The control group, transfected with empty plasmid, showed no apoptotic features. Scale bar = 100 μm. (C) Overexpression of *Sp*-caspase promoting apoptosis in HEK293T cells was detected with Annexin V-FITC/Hoechst staining. Scale bar = 20 μm. (D) Overexpression of *Sp*-caspase promoting apoptosis in HEK293T cells was detected by TUNEL assay. Scale bar = 50 μm.

thus more apoptosis-related components need to be identified, which will contribute to the study of its mechanism. Secondly, *Sp-caspase* is an effector caspase, however the initiator caspase has not been identified. Therefore, how *Sp-caspase* is activated is obscure. Thirdly, the molecular function of *Sp-caspase* in the innate immune response still requires further study. All these studies of apoptosis in crustaceans will contribute to diseases control in mud crab farming industry.

Authors contributions

Jishan Li: Designing research work, Performing experiments, Writing - original draft, Revising manuscript. **Lixia Dong:** Designing research work, Performing experiments. **Depeng Zhu:** Performing experiments. **Min Zhang:** Performing experiments. **Kejian Wang:** Designing research work, Revising manuscript, Funding acquisition. **Fangyi Chen:** Designing research work, Performing experiments, Revising manuscript, Funding acquisition.

Acknowledgements

This study was supported by Fundamental Research Funds for the Central Universities of China (Grant # 20720180100/20720180117). We thank to laboratory engineer Huiyun Chen for providing technical assistance in confocal microscopy imaging. We also thank Dr. Changchuan Xie and Yaying Wu (School of Life Sciences, Xiamen University) for mass spectrometry analysis.

Appendix A. Supplementary data

Supplementary data to this article can be found online at https://doi.org/10.1016/j.fsi.2020.05.045.

References

[1] J.C. Reed, K.S. Doctor, A. Godzik, The domains of apoptosis: a genomics perspective, Sci. STKE 2004 (2004) re9.
[2] P.F. Connolly, H.O. Fearnhead, Viral hijacking of host caspases: an emerging category of pathogen–host interactions, Cell Death Differ. 24 (2017) 1401–1410.
[3] S. Wilk, Teaching resources, Apoptosis, Sci. STKE. 2005 (2005) tr16.
[4] A.M. Scott, M. Saleh, The inflammatory caspases: guardians against infections and sepsis, Cell Death Differ. 14 (2007) 23–31.
[5] O. Julien, J.A. Wells, Caspases and their substrates, Cell Death Differ. 24 (2017) 1380–1389.
[6] P. Clarke, K.L. Tyler, Apoptosis in animal models of virus-induced disease, Nat. Rev. Microbiol. 7 (2009) 144–155.
[7] N.A. Thornberry, Y. Lazebnik, Caspases: enemies within, Science 281 (1998) 1312–1316.
[8] A. Degterev, M. Boyce, J. Yuan, A decade of caspases, Oncogene 22 (2003) 8543–8567.
[9] H. Chen, X. Ning, Z. Jiang, Caspases control antiviral innate immunity, Cell. Mol. Immunol. 14 (2017) 736–747.
[10] S. Shalini, L. Dorstyn, S. Dawar, S. Kumar, Old, new and emerging functions of caspases, Cell Death Differ. 22 (2015) 526–539.
[11] A.S. Tseng, D.S. Adams, D. Qiu, P. Koustubhan, et al., Apoptosis is required during early stages of tail regeneration in *Xenopus laevis*, Dev. Biol. 301 (2007) 62–69.
[12] K. Nakajima, A. Takahashi, Y. Yaoita, Structure, expression, and function of the *Xenopus laevis* caspase family, J. Biol. Chem. 275 (2000) 10484–10491.
[13] O. Spead, T. Verreet, C.J. Donelson, F.E. Poulain, Characterization of the caspase family in zebrafish, PloS One 13 (2018) e0197966.
[14] N. Inohara, G. Nunez, Genes with homology to mammalian apoptosis regulators

identified in zebrafish, Cell Death Differ. 7 (2000) 509–510.
[15] X. Wang, C. Yang, Programmed cell death and clearance of cell corpses in *Caenorhabditis elegans*, Cell. Mol. Life Sci. 73 (2016) 2221–2236.
[16] S. Kumar, J. Doumanis, The fly caspases, Cell Death Differ. 7 (2000) 1039–1044.
[17] S. Kornbluth, K. White, Apoptosis in *Drosophila*: neither fish nor fowl (nor man, nor worm), J. Cell Sci. 118 (2005) 1779–1787.
[18] S. Fu, M. Ding, Y. Yang, J. Kong, et al., Molecular cloning, characterization and expression analysis of caspase-6 in puffer fish (*Takifugu obscurus*), Aquaculture 490 (2018) 311–320.
[19] S. Fu, M. Ding, H. Liu, L. Wu, et al., Identification and characterization of caspase-7 in pufferfish (*Takifugu obscurus*) in response to bacterial infection and cell apoptosis, Aquaculture 512 (2019) 734268.
[20] M. Li, Y. Ding, Y. Mu, J. Ao, et al., Molecular cloning and characterization of caspase-3 in large yellow croaker (*Pseudosciaena crocea*), Fish Shellfish Immunol. 30 (2011) 910–916.
[21] Y. Mu, X. Xiao, J. Zhang, J. Ao, et al., Molecular cloning and functional characterization of caspase 9 in large yellow croaker (*Pseudosciaena crocea*), Dev. Comp. Immunol. 34 (2010) 300–307.
[22] D.A. Elvitigala, I. Whang, H.K. Premachandra, N. Umasuthan, et al., Caspase 3 from rock bream (*Oplegnathus fasciatus*): genomic characterization and transcriptional profiling upon bacterial and viral inductions, Fish Shellfish Immunol. 33 (2012) 99–110.
[23] H. Long, L. Sun, Molecular characterization reveals involvement of four caspases in the antibacterial immunity of tongue sole (*Cynoglossus semilaevis*), Fish Shellfish Immunol. 57 (2016) 340–349.
[24] L. Ren, R. Wang, T. Xu, Three representative subtypes of caspase in miiuy croaker: genomic organization, evolution and immune responses to bacterial challenge, Fish Shellfish Immunol. 40 (2014) 61–68.
[25] A. Yan, C. Ren, T. Chen, D. Huo, et al., A novel caspase-6 from sea cucumber *Holothuria leucospilota*: molecular characterization, expression analysis and apoptosis detection, Fish Shellfish Immunol. 80 (2018) 232–240.
[26] A. Yan, C. Ren, T. Chen, X. Jiang, et al., The first tropical sea cucumber caspase-8 from *Holothuria leucospilota*: molecular characterization, involvement of apoptosis and inducible expression by immune challenge, Fish Shellfish Immunol. 72 (2018) 124–131.
[27] Y. Shao, Z. Che, C. Li, W. Zhang, et al., A novel caspase-1 mediates inflammatory responses and pyroptosis in sea cucumber *Apostichopus japonicus*, Aquaculture 513 (2019) 734399.
[28] G. Lu, Z. Yu, M. Lu, D. Liu, et al., The self-activation and LPS binding activity of executioner caspase-1 in oyster *Crassostrea gigas*, Dev. Comp. Immunol. 77 (2017) 330–339.
[29] J. Xu, S. Jiang, Y. Li, M. Li, et al., Caspase-3 serves as an intracellular immune receptor specific for lipopolysaccharide in oyster *Crassostrea gigas*, Dev. Comp. Immunol. 61 (2016) 1–12.
[30] W. Huang, H. Ren, S. Gopalakrishnan, D. Xu, et al., First molecular cloning of a molluscan caspase from variously colored abalone (*Haliotis diversicolor*) and gene expression analysis with bacterial challenge, Fish Shellfish Immunol. 28 (2010) 587–595.
[31] K. Wongprasert, P. Sangsuriya, A. Phongdara, S. Senapin, Cloning and characterization of a caspase gene from black tiger shrimp (*Penaeus monodon*)-infected with white spot syndrome virus (WSSV), J. Biotechnol. 131 (2007) 9–19.
[32] T. Lertwimol, P. Sangsuriya, K. Phiwsaiya, S. Senapin, et al., Two new anti-apoptotic proteins of white spot syndrome virus that bind to an effector caspase (PmCasp) of the giant tiger shrimp *Penaeus (Penaeus) monodon*, Fish Shellfish Immunol. 38 (2014) 1–6.
[33] J. Leu, H. Wang, G. Kou, C. Lo, *Penaeus monodon* caspase is targeted by a white spot syndrome virus anti-apoptosis protein, Dev. Comp. Immunol. 32 (2008) 476–486.
[34] L. Wang, B. Zhi, W. Wu, X. Zhang, Requirement for shrimp caspase in apoptosis against virus infection, Dev. Comp. Immunol. 32 (2008) 706–715.
[35] H. Zuo, C. Chen, Y. Gao, J. Lin, et al., Regulation of shrimp PjCaspase promoter activity by WSSV VP38 and VP41B, Fish Shellfish Immunol. 30 (2011) 1188–1191.
[36] A. Phongdara, W. Wanna, W. Chotigeat, Molecular cloning and expression of caspase from white shrimp *Penaeus merguiensis*, Aquaculture 252 (2006) 114–120.
[37] P. Wang, D. Wan, Y. Chen, S. Weng, et al., Characterization of four novel caspases from *Litopenaeus vannamei* (Lvcaspase2-5) and their role in WSSV infection through dsRNA-mediated gene silencing, PloS One 8 (2013) e80418.
[38] X. Jin, W. Li, L. He, W. Lu, et al., Molecular cloning, characterization and expression analysis of two apoptosis genes, caspase and nm23, involved in the antibacterial response in Chinese mitten crab, *Eriocheir sinensis*, Fish Shellfish Immunol. 30 (2011) 263–272.
[39] M. Wu, X. Jin, A. Yu, Y. Zhu, et al., Caspase-mediated apoptosis in crustaceans: cloning and functional characterization of EsCaspase-3-like protein from *Eriocheir sinensis*, Fish Shellfish Immunol. 41 (2014) 625–632.
[40] X. Ren, X. Yu, B. Gao, P. Liu, et al., Characterization of three caspases and their pathogen-induced expression pattern in *Portunus trituberculatus*, Fish Shellfish Immunol. 66 (2017) 189–197.
[41] F. Chen, K. Wang, Characterization of the innate immunity in the mud crab *Scylla paramamosain*, Fish Shellfish Immunol. 93 (2019) 436–448.
[42] S.P. Wang, F.Y. Chen, L.X. Dong, Y.Q. Zhang, et al., A novel innexin2 forming membrane hemichannel exhibits immune responses and cell apoptosis in *Scylla paramamosain*, Fish Shellfish Immunol. 47 (2015) 485–499.
[43] E. Ortona, P. Matarrese, W. Malorni, Taking into account the gender issue in cell death studies, Cell Death Dis. 5 (2014) e1121.
[44] D.G. Monroe, R.R. Berger, M.M. Sanders, Tissue-protective effects of estrogen involve regulation of caspase gene expression, Mol. Endocrinol. 16 (2002) 1322–1331.
[45] Y. Zhang, O. Tounekti, B. Akerman, C.G. Goodyer, et al., 17-beta-estradiol induces an inhibitor of active caspases, J. Neurosci. 21 (2001) RC176.
[46] P.G. Bradford, K.V. Gerace, R.L. Roland, B.G. Chrzan, Estrogen regulation of apoptosis in osteoblasts, Physiol. Behav. 99 (2010) 181–185.
[47] H.G. Patterton, S. Graves, DNAssist: the integrated editing and analysis of molecular biology sequences in Windows, Bioinformatics 16 (2000) 652–653.
[48] K. Tamura, G. Stecher, D. Peterson, A. Filipski, et al., MEGA6: molecular evolutionary genetics analysis version 6.0, Mol. Biol. Evol. 30 (2013) 2725–2729.
[49] K.J. Livak, T.D. Schmittgen, Analysis of relative gene expression data using real-time quantitative PCR and the 2(-Delta Delta C(T)) Method, Methods 25 (2001) 402–408.
[50] A.M. Lackie, Invertebrate immunity, Parasitology 80 (2009) 393–412.
[51] Y. Xu, W. Yang, Roles of three Es-Caspases during spermatogenesis and Cadmium-induced apoptosis in *Eriocheir sinensis*, Aging 10 (2018) 1146–1165.
[52] C. Qu, W. Yang, Q. Xu, J. Sun, et al., A novel effector caspase (caspase-3/7-1) involved in the regulation of immune homeostasis in Chinese mitten crab *Eriocheir sinensis*, Fish Shellfish Immunol. 83 (2018) 76–83.
[53] S. Sun, F. Xuan, H. Fu, J. Zhu, et al., Molecular cloning, characterization and expression analysis of caspase-3 from the oriental river prawn, *Macrobrachium nipponense* when exposed to acute hypoxia and reoxygenation, Fish Shellfish Immunol. 62 (2017) 291–302.
[54] Y. Shao, C. Li, W. Zhang, X. Duan, et al., Molecular cloning and characterization of four caspases members in *Apostichopus japonicus*, Fish Shellfish Immunol. 55 (2016) 203–211.
[55] J. Arockiaraj, S. Easwvaran, P. Vanaraja, A. Singh, et al., Effect of infectious hypodermal and haematopoietic necrosis virus (IHHNV) infection on caspase 3c expression and activity in freshwater prawn *Macrobrachium rosenbergii*, Fish Shellfish Immunol. 32 (2012) 161–169.
[56] R. Wang, Y. Zhong, X. Gu, J. Yuan, et al., The pathogenesis, detection, and prevention of *Vibrio parahaemolyticus*, Front. Microbiol. 6 (2015) 144.
[57] K. Alagappan, V. Karuppiah, B. Deivasigamani, Protective effect of phages on experimental *V. parahaemolyticus* infection and immune response in shrimp (Fabricius, 1798), Aquaculture 453 (2016) 86–92.
[58] T. Marudhupandi, T.T.A. Kumar, S. Prakash, J. Balamurugan, et al., *Vibrio parahaemolyticus* a causative bacterium for tail rot disease in ornamental fish, *Amphiprion sebae*, Aquacult Rep 8 (2017) 39–44.
[59] H. Liu, Y. Wang, J. Cao, H. Jiang, et al., Antimicrobial activity and virulence attenuation of citral against the fish pathogen *Vibrio alginolyticus*, Aquaculture 515 (2020) 734578.
[60] Y. Zhou, W. Gu, D. Tu, Q. Zhu, et al., Hemocytes of the mud crab *Scylla paramamosain*: cytometric, morphological characterization and involvement in immune responses, Fish Shellfish Immunol. 72 (2018) 459–469.
[61] M. Ahmad, S.M. Srinivasula, L.J. Wang, G. Litwack, et al., *Spodoptera frugiperda* caspase-1, a novel insect death protease that cleaves the nuclear immunophilin FKBP46, is the target of the baculovirus antiapoptotic protein p35, J. Biol. Chem. 272 (1997) 1421–1424.
[62] Z. Song, K. McCall, H. Steller, DCP-1, a *Drosophila* cell death protease essential for development, Science 275 (1997) 536–540.